Available online at www.sciencedirect.com
ScienceDirect
Ceramics International 35 (2009) 2343–2350
CERAMICS INTERNATIONAL
www.elsevier.com/locate/ceramint

Preparation, biomimetic apatite induction and osteoblast proliferation test of TiO_2-based coatings containing P with a graded structure

Daqing Wei *, Yu Zhou

Institute for Advanced Ceramics, Harbin Institute of Technology, Harbin 150001, PR China

Received 3 November 2008; received in revised form 21 November 2008; accepted 21 January 2009
Available online 6 February 2009

Abstract

TiO_2-based coatings containing P (T–P) were prepared on Ti6Al4V by microarc oxidation (MAO) with applied voltages of 200–400 V in an electrolyte containing $(NaPO_3)_6$ and NaOH. The surfaces of the T–P coatings became rough and the thickness increased with increasing the applied voltage. Above 200 V, anatase was found on the surface, and rutile was observed at 400 V. With increasing the coating thickness, the O and P concentrations increase; while Ti and Al concentrations decrease. Ti, O and P elements display a uniform distribution character around the micropores on the surface of the T–P coating formed at 300 V. However, the inner of the micropores exhibits a high Ti concentration and low O and P concentrations due to the graded distributions of Ti, O and P elements in the T–P coating. The apatite-forming ability of the T–P coating formed at 300 V was evaluated by immersing in a simulated body fluid (SBF) for 28 and 56 days. The results indicate that biomimetic apatite was formed on the surface of the T–P coating after immersion in SBF for 56 days. And the further cell experiment indicates that the T–P coating can provide surface suitable for the MG63 cell proliferation.

Keywords: B. Surfaces; D. TiO_2; Microarc oxidation; Biomimetic apatite; Cell proliferation

1. Introduction

Titanium and its alloys are important biomedical materials in skeletal repair and dental implants area [1]. They possess excellent mechanical strength, toughness, biocompatibility and corrosion resistance, leading to widespread clinical success [1]. However, titanium and its alloys show a bioinert nature. One approach to overcoming the disadvantage of titanium and its alloys is to produce bioactive ceramic coatings on their surfaces [1]. Many surface modifying techniques such as plasma spraying [2,3], sol–gel method [4], and electrochemical deposition [5] have been developed to prepare bioactive ceramic coatings such as calcium phosphate and glass–ceramic on titanium and its alloys.

In recent years, TiO_2-based coatings containing Ca and P (T–CaP) have gained much attention for constructing this bioactive surface [6–17]. These coatings can be easily formed on titanium and its alloys by a relatively convenient and effective technique of microarc oxidation (MAO) [6–17]. Normally, in the MAO process the electrolytes were composed of calcium salts and phosphates such as calcium acetate (CA), EDTA-Ca chelate complex, calcium glycerophosphate (Ca–GP) and calcium dihydrogen phosphate, etc. [6–17]. Besides T–CaP coating, recently, the structure and apatite-forming ability of the TiO_2-based coatings formed in electrolyte only containing phosphates or calcium salts are noticed by researchers. Hong and co-workers [18] used the MAO technique to prepare TiO_2-based coating containing Ca (T–Ca) on titanium in an electrolyte containing CA. However, no apatite was induced on this coating during the testing process. Besides T–Ca coating, TiO_2-based coating containing P (T–P) has also been noticed [19]. In recent study [19], an electrolyte containing β-glycerol phosphate disodium salt pentahydrate (β-GP, $C_3H_7Na_2O_6P{\cdot}5H_2O$) was used to prepare T–P coating

* Corresponding author at: P.O. Box 433, Department of Materials Science and Engineering, Harbin Institute of Technology, Harbin 150001, PR China. Tel.: +86 451 8640 2040 8511; fax: +86 451 8641 4291.
E-mail address: daqingwei@hit.edu.cn (D. Wei).

0272-8842/$34.00
doi:10.1016/j.ceramint.2009.01.007

by MAO technique. The results also indicated that no apatite was formed on the surface of this T–P coating during SBF immersion process. And subsequent hydrothermal treatment was recommended to treat this coating for improving its apatite-forming ability. In this work, T–P coatings were prepared by MAO in an electrolyte containing $(NaPO_3)_6$ and NaOH. The current results indicated that this T–P coating has apatite-forming ability in SBF and shows good property of cell proliferation.

2. Materials and methods

2.1. Microarc oxidation

In the MAO process, Ti6Al4V plates (10 mm × 10 mm × 1.5 mm) were polished with SiC abrasive papers, ultrasonically cleaned with acetone and distilled water, and dried at 40 °C. The Ti6Al4V plates were used as anodes and stainless steel plates were used as cathodes in an electrolytic bath. The distance between the anode and cathode was about 15 cm. A fresh electrolyte prepared by dissolving reagent-grade chemicals of $(NaPO_3)_6$ (20 g/l) and NaOH (10 g/l) into deionized water was used for the MAO process. The applied voltage, frequency, duty cycle and oxidizing time were 300 V, 600 Hz, 8.0% and 5 min, respectively. The temperature of the electrolyte was kept at 40 °C by a cooling system.

2.2. Immersion of the samples in a simulated body fluid

The T–P samples were soaked in 15 mL SBF [20] (Table 1), immersing for different time, and the SBF was refreshed every other day. The SBF was prepared by dissolving reagent-grade chemicals of NaCl, $NaHCO_3$, KCl, $K_2HPO_4{\cdot}3H_2O$, $MgCl_2{\cdot}6H_2O$, $CaCl_2$, and Na_2SO_4 into deionized water and buffering at pH 7.40 with tris-hydroxymethylaminomethane ($(CH_2OH)_3CNH_2$) and 1.0 mol/L HCl at 37 °C.

2.3. X-ray diffraction

The T–P coatings before and after immersion in the SBF, the phase composition of the sample surfaces were analyzed by a grazing-incidence X-ray diffraction (XRD, Philips X'Pert, Holland) using a Cu Kα radiation. In the XRD experiment, the angle of the incident beam was fixed at 1° against the sample surfaces in order to detect the phase composition of the sample surfaces and the measurements were performed with a continuous scanning mode at a rate of 2° min^{-1}.

Table 1
Ion concentrations of SBF and human blood plasma.

Ion	Concentrations (mmol/L)	
	SBF	Blood plasma
Na^+	142.0	142.0
K^+	5.0	5.0
Mg^{2+}	1.5	1.5
Ca^{2+}	2.5	2.5
Cl^-	147.8	103.8
HCO_3^{2-}	4.2	27
HPO_4^{2-}	1.0	1.0
SO_4^{2-}	0.5	0.5

2.4. Scanning electron microscopy and energy dispersive X-ray spectrometer

The surface morphologies of the samples were observed by a scanning electron microscopy (SEM, CamScan MX2600, CamScan Co., England). In addition, the ion concentrations of the sample surfaces were detected by an energy dispersive X-ray spectrometer (EDS, Oxford Model 7537, England) equipped on the SEM system.

2.5. X-ray photoelectron spectroscopy

An X-ray photoelectron spectroscopy (XPS, PHI 5700, America physical electronics) was used to detect the chemical compositions of the T–P coating formed at 300 V after SBF incubation for 56 days. An Al Kα (1486.6 eV) X-ray source was used to analyze the chemical states of Ca and P with a hemispherical analyzer in a high-resolution mode. The XPS take-off angle was set at 45°. A region about 2 mm × 0.8 mm on each surface was analyzed. The measured binding energies were calibrated by the C1s (hydrocarbon C–C, C–H) of 285 eV.

2.6. Fourier transform infrared spectroscopy

Fourier transform infrared spectroscopy (FT-IR, Bruker Vector 22, Germany) was also used to analyze the structure of the T–P coating formed at 300 V after SBF incubation for 56 days. In the FT-IR experiment, the resolution and scanning range were 4 and 4000–400 cm^{-1}, respectively.

2.7. Biological properties

The biological properties of the samples were evaluated by preliminary in vitro cell tests. In the cell tests, the MG63 were used to characterize the proliferation behavior of the cells. The pre-incubated cell lines were plated onto specimens with a cell density of 2×10^4 mL^{-1}, and then cultured in a humidified incubator with 5% CO_2 at 37 °C. Dulbecco's modified Eagle's medium (DMEM) with 10% fetal bovine serum (FBS) was used as the culturing medium. The proliferation behavior was determined by counting the number of cells after culturing them for 5 and 7 days. The cells were detached from the samples with 0.05% trypsin-EDTA and counted using a hemocytometer. To observe the morphology of the proliferated cells by SEM, the cultured samples were fixed by 4% paraformaldehyde for 20 min.

2.8. Statistical analysis

The experimental data were represented as means ± one standard deviations (S.D.) for $n = 5$. Statistical analysis was conducted via a one-way analysis of variance.

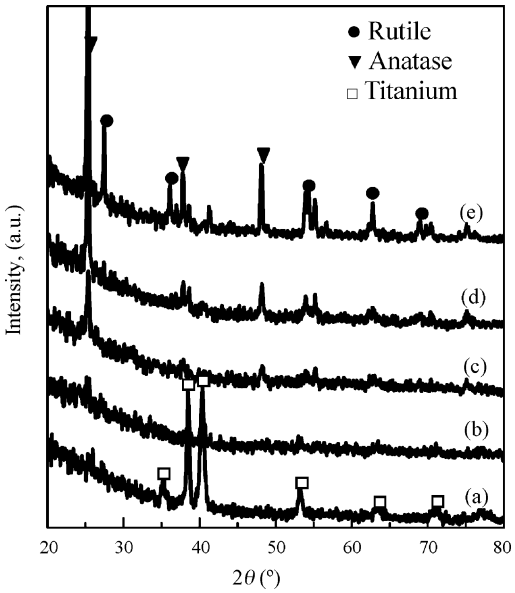

Fig. 1. XRD patterns of the T–P coatings formed at various applied voltages: (a) 200 V, (b) 250 V, (c) 300 V, (d) 350 V and (e) 400 V.

3. Results and discussion

3.1. Characteristics of the T–P coatings

The XRD patterns of the T–P coatings formed at 200–400 V are shown in Fig. 1. At low applied voltages (200 and 250 V), diffraction peaks of Ti were detected. Above 250 V, the diffraction peaks of anatase were found and Ti peaks disappeared. In addition, rutile was observed at 400 V. As well known, anatase is stable at low temperature and rutile is stable at high temperature. Thus, rutile was produced due to high energy provided by MAO equipment when high applied voltages were used.

The surface morphologies of the T–P coatings formed at various voltages (200–400 V) are shown in Fig. 2. No evident micropore character was observed at 200 V. Above 200 V the T–P coatings exhibit a porous structure. Critical applied voltage

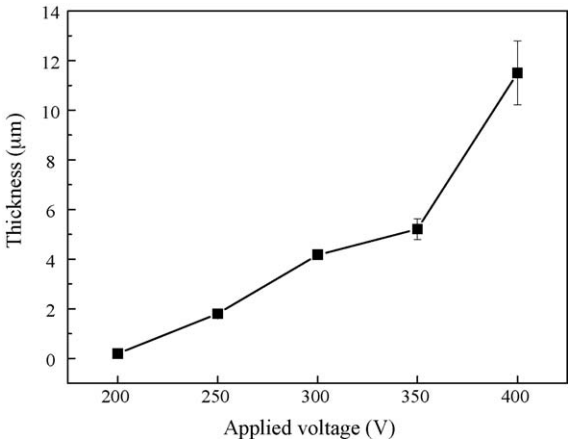

Fig. 3. The thickness of the T–P coatings formed at various applied voltages: (a) 200 V, (b) 250 V, (c) 300 V, (d) 350 V and (e) 400 V.

is necessary for forming the T–P coatings [21]. The micropores are distributed at regular intervals at 300 and 350 V with diameters in ∼3 μm. At 400 V the surfaces of the T–P coatings become rough and irregular. The results indicate that the applied voltage has a significant effect on the surface morphology of the T–P coating in the present electrolyte.

The thickness of the T–P coating is measured as a function of the applied voltage through SEM observation. As expected, the thickness of the T–P coating increases with increasing the applied voltage (Fig. 3). SEM micrographs of the cross-sections of the T–P coatings are shown in Fig. 4. No apparent discontinuity between the coatings and substrates was observed at various applied voltages (250–400 V) (Fig. 4(a)–(d)), suggesting the T–P coatings with good interfacial bonding to the substrate.

The major surface constituents found for the T–P coatings are O, Ti, P, Na and C according to the EDS results. Under the applied voltage, the initial passivating coating on the surface of titanium alloy was broken yielding microarc discharge, and a discharge channel was formed [21]. Thus, the electrolyte can flow into the discharge channel, and the titanium alloy substrate can contact the electrolyte. During the microarc discharge

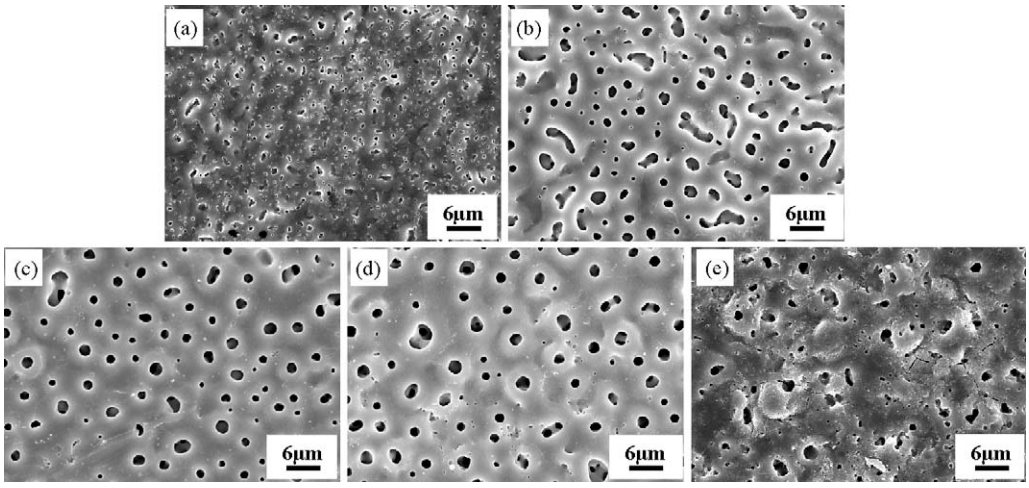

Fig. 2. Surface morphologies of the T–P coatings formed at various applied voltages: (a) 200 V, (b) 250 V, (c) 300 V, (d) 350 V and (e) 400 V.

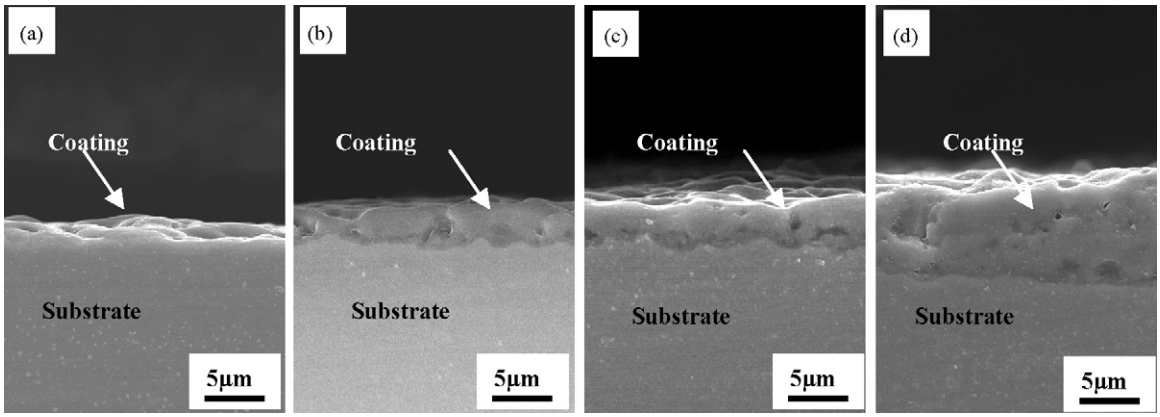

Fig. 4. SEM micrographs of the cross-section of the T–P coatings formed at various applied voltages: (a) 250 V, (b) 300 V, (c) 350 V and (d) 400 V.

process, intensive plasma physical and chemical reactions occur in the discharge channel, companied with a high pressure and a high temperature condition. Then, lots of Ti near the surface of the titanium alloy substrate would participate in the subsequent reactions and be oxidized to form TiO_2. Moreover, the negatively charged phosphate radical ions move to the anode easily in the electrolyte under the applied electric field. Thus, P was introduced into the T–P coatings.

Fig. 5 shows the elemental distributions of the cross-section of the T–P coating. All the elements show graded distribution along the coating depth. With increasing the coating thickness, the O and P concentrations increase; while the Ti and Al concentrations decrease. Actually, a coating with a graded structure is usually favored due to its mechanical stability and good match regarding crystallographic structure and the thermal expansion coefficients between coating and substrate [22].

Fig. 6 shows the elemental distributions on the surfaces of the T–P coating determined by EDS. It can be seen that the Ti, O and P elements display a uniform distribution character around the micropores (Fig. 6). However, the inner of the micropores exhibits a high Ti concentration and low O and P concentrations. As mentioned above, the concentration of Ti is high near the titanium substrate in the T–P coating. Thus, it was not difficult to understand that the concentration of Ti is high in the micropores since these sites are near the titanium substrate. Similar results were observed on the surfaces of the TiO_2-based coatings containing Ca and P [8]. According to the above

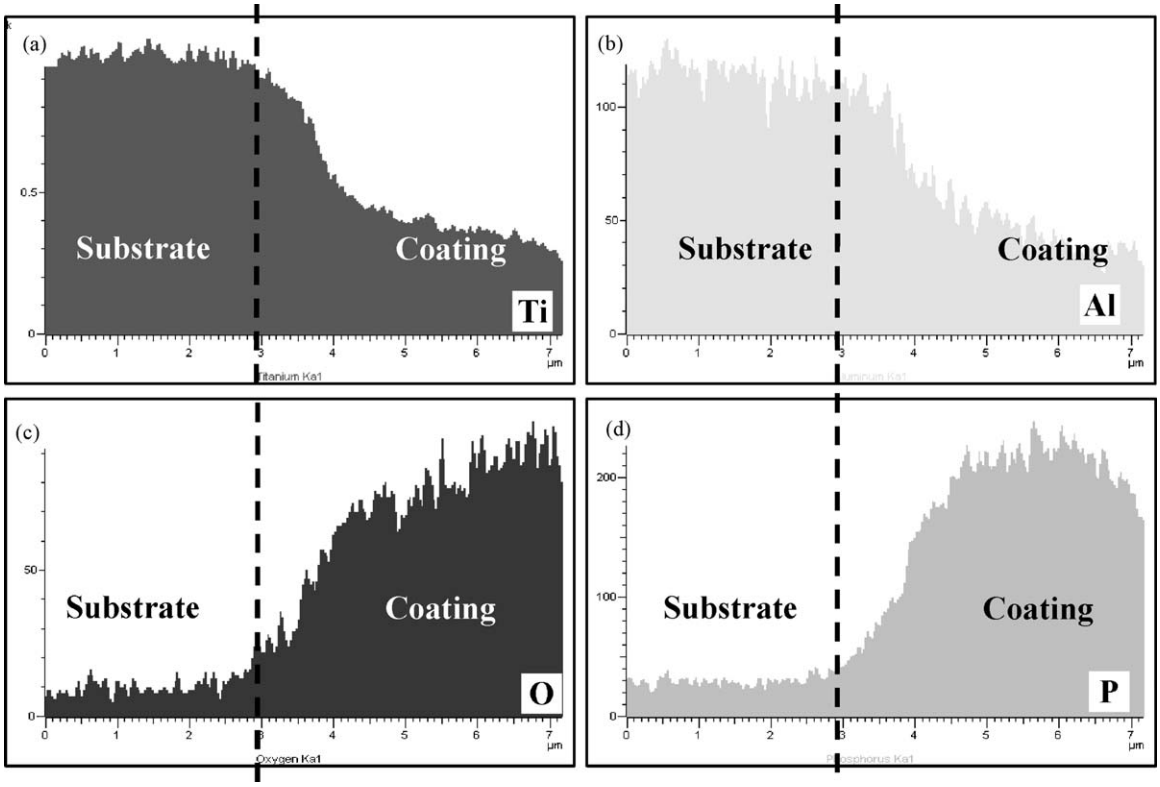

Fig. 5. Elemental distribution of the cross-section of the T–P coating formed at 300 V: (a) Ti, (b) Al, (c) O and (d) P distribution.

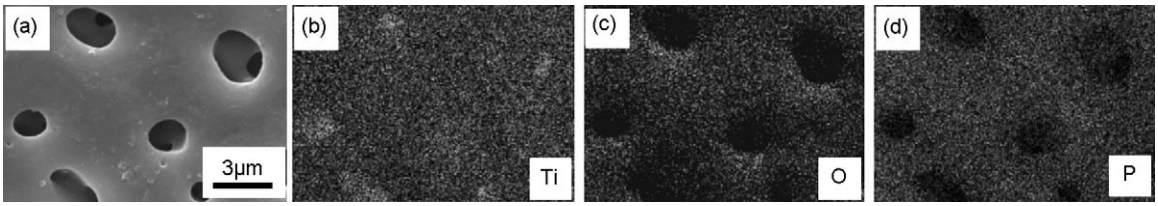

Fig. 6. Elemental distribution on the surface of the T–P coating formed at 300 V determined by EDS: (a) surface morphology, (b) Ti, (c) O and (d) P distribution.

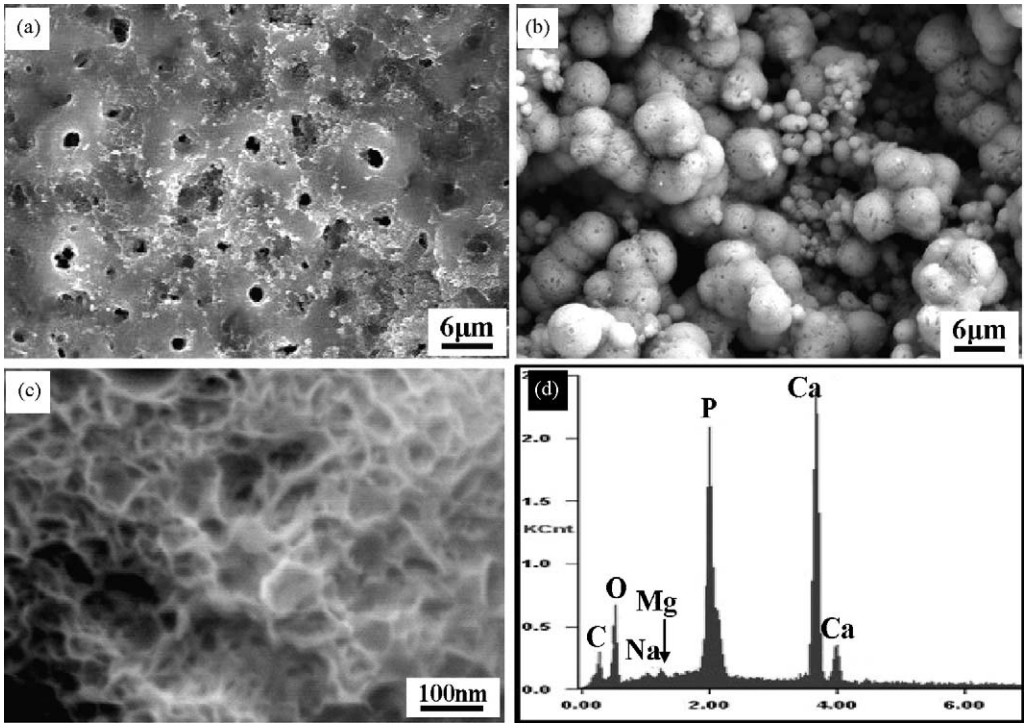

Fig. 7. Surface morphology and EDS spectrum of the T–P coating formed at 300 V after SBF immersion: (a) 28 days, (b) 56 days, (c) higher magnification of (b) and (f) EDS result of the (d).

results, it was indicated that the phase and surface structure changes are closely related to the applied voltage.

3.2. Biomimetic apatite on the T–P coating

The surface morphologies of the T–P coating after soaking in the SBF for 28 and 56 days are shown in Fig. 7. After 28 days, the surface of the T–P coating was slightly modified and the porous structure of the T–P coating can be distinguished yet (Fig. 7(a)). Further increasing the SBF immersion time to 56 days, the entire surface of the T–P coating was covered a new coating showing numerous sphere-like precipitates with diameters ~5 μm (Fig. 7(b)). At a higher magnification, it was found that the new coating possesses a network structure mainly composed of nano-scale crystals (Fig. 7(c)). The EDS results further indicate that the new layer was composed of Ca- and P-containing (CP) precipitates (Fig. 7(d)). In addition, Na and Mg elements were detected in the CP phase, which agrees with the results of Müller and Müller [23].

The XRD result further indicates that the CP precipitate on the surface of the T–P coating was apatite (Fig. 8), indicating that the T–P coating has apatite-forming ability.

Fig. 9 shows the FT-IR spectrum of the T–P coating after soaking in the SBF for 56 days. The SBF-treated T–P coating shows the broad absorption bands of H_2O at 3451 and 1650 cm^{-1}. The spectrum clearly illustrate the PO_4 at 1030, 600 and 561 cm^{-1} and double degenerated bending mode of ν_2PO_4 bands at 470 cm^{-1} [23,24]. In the FT-IR spectrum, the CO_3^{2-} absorption bands also were observed including bending

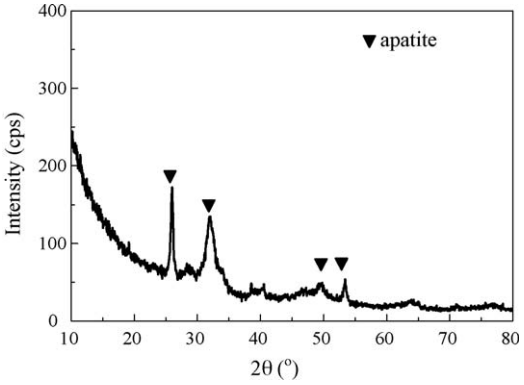

Fig. 8. XRD pattern of the T–P coating formed at 300 V after SBF immersion for 56 days.

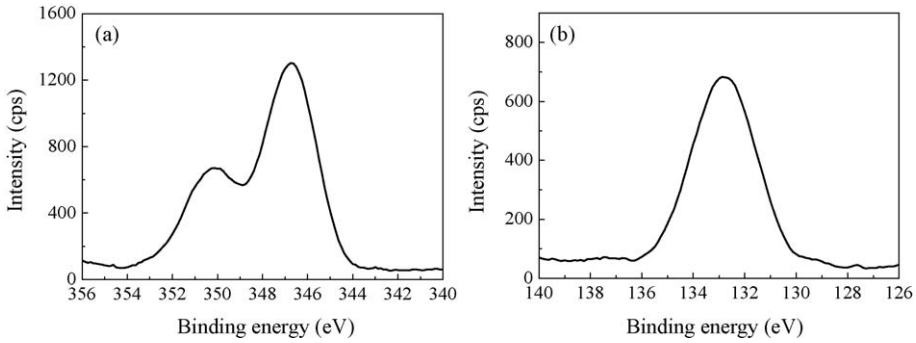

Fig. 9. XPS spectra of (a) Ca2p and (b) P2p of the surfaces of the T–P coating formed at 300 V after SBF immersion for 56 days.

mode of the $\nu_4CO_3^{2-}$ group in A-type carbonated HA (CHA) at 1552 cm^{-1}, characteristic stretching mode of $\nu_3CO_3^{2-}$ group in CHA at 1502 cm^{-1}, characteristic stretching mode of $\nu_1CO_3^{2-}$ group in A-type CHA at 1566 cm^{-1}, stretching mode of $\nu_1CO_3^{2-}$ group in B-type CHA at 1428 cm^{-1} and bending mode of (ν_3 or ν_4) CO_3^{2-} group in CHA at 871 cm^{-1} [23,24]. In addition, the characteristic peaks at 1102, 952 and 871 cm^{-1} also suggest the presence of HPO_4^{2-} in the apatite, according to the reported results [23,24]. The results indicate that the T–P coating can induce the formation of carbonated apatite, which is similar to biological apatites.

Fig. 10 shows the XPS spectra of Ca2p and P2p of the T–P coating after SBF incubation for 56 days. Ca2p spectrum shows a doublet at 346.6 and 350.21 eV and P2p spectrum reveals single peak at 132.9 eV. These BE values are agree well with the previous results of carbonated HA obtained by biomimetic method [17].

Compared to synthetic HA, biological apatites possess different physical and chemical properties because of substitutions and hence differences in composition. Thus, investigators attempted to obtain biological apatites by artificial synthesis method. In this process, biomimetic technique is an important method to obtain artificial apatites similar biological apatites. It is derived from the inspiration of biomineralization, which is a natural biological apatite formation process [25]. This technique possesses some advantages such as low working temperature, accessibility of pore networks on the nanometer scale and suitability for complex shapes of substrates [26–34]. Moreover, biomimetic apatite presents some important characteristics such as carbonated structure and controllable crystallinity [23]. In addition, this method provides a probability of co-depositing biological macromolecules such as various proteins.

To obtain biomimetic apatite, layers that are capable of inducing apatite deposition should be established on substrates. And then, the modified substrates were immersed in simulated body fluid (SBF) to induce the apatite formation. Anatase may is a chemical stimulus for the bonelike apatite formation on biomaterial surface in SBF. As reported, the iso-electric point of anatase is 5.9 ± 0.2 [35]. Thus, a negatively charged surface will be formed on the T–P coating in the SBF with a pH 7.4. As a result, this surface can incorporate calcium ions due to electrostatic force, and then absorb the phosphate radicals and carbonic acid ions. Therefore, the suitable iso-electric point of anatase may acts as the chemical stimulus for bonelike apatite formation. In fact, the investigation of Wu and Nancollas indicated that apatite could be absorbed on the surface of TiO_2 [36]. The previous result indicated the presence of the P–O group in the T–P coating [37]. Generally, substrates with functionalized surfaces such as –OH, PO_4H_2, COOH, SO_3H, and $CONH_2$ groups, etc. facilitate the formation of bonelike apatite in SBF or solutions containing various ions with respect to apatite [25]. The P–O group of the T–P coating may be the other factor to induce the apatite formation, which needs a more through investigation in the future.

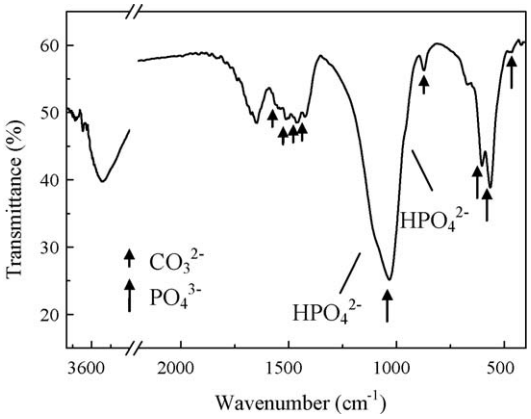

Fig. 10. FT-IR spectrum of the T–P coating formed at 300 V after soaking in the SBF for 56 days.

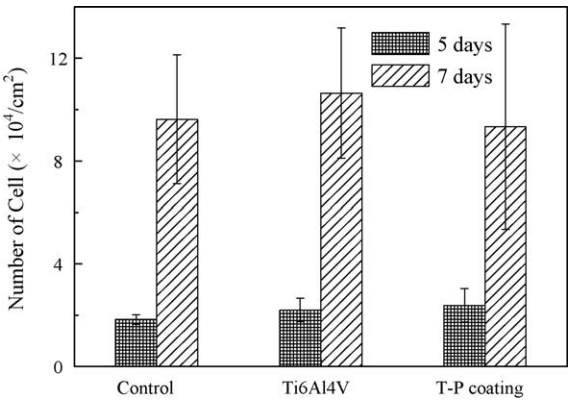

Fig. 11. Number of MG63 cells after proliferation for 5 and 7 days on the surfaces of control, Ti6Al4V and T–P coating formed at 300 V.

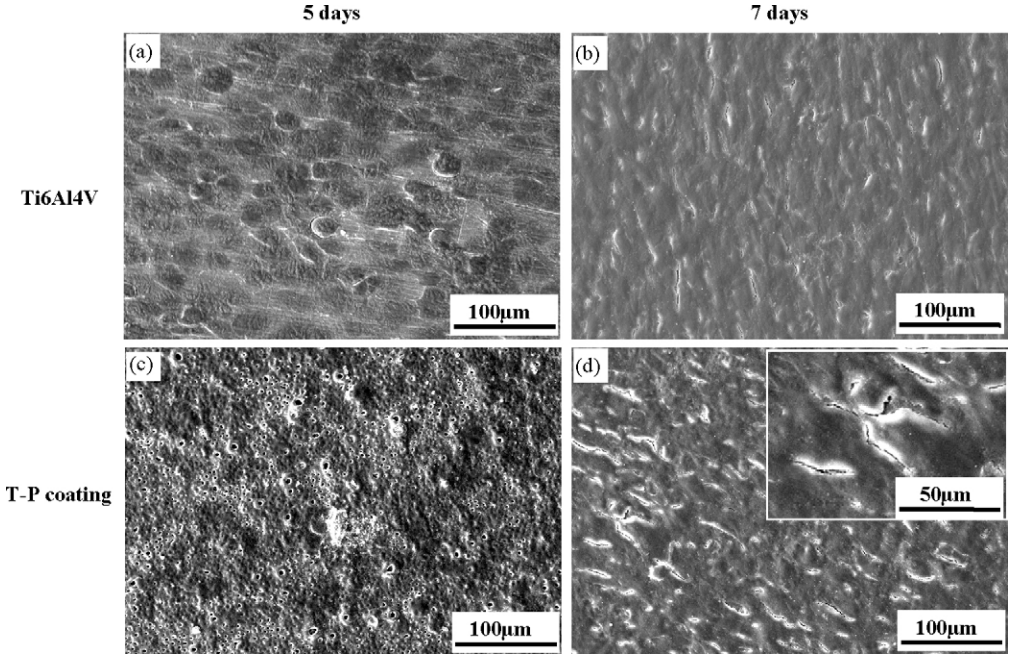

Fig. 12. SEM morphology of MG63 cells after culturing for 5 and 7 days on the Ti6Al4V and T–P coatings formed at 300 V: (a) and (b) on Ti6Al4V culturing for 5 and 7 days and (c) and (d) on T–P coating culturing for 5 and 7 days.

3.3. Cell proliferation

In this work, preliminary investigation of the MG63 cell proliferation on the surface of the T–P coating was conducted. After culturing 5 and 7 days, the cells proliferated on the surfaces of the control samples, titanium alloy and T–P coatings formed at 300 V were counted, as shown in Fig. 11. Compared with the control samples, the effects of titanium alloy and T–P coatings on the cell proliferation were no significant difference ($p > 0.005$). This result indicated that the proliferation of MG63 cells is good on the T–P coatings. The MG63 cells can proliferate on the titanium alloy surface probably due to the presence of a hydroxide-oxide which has formed by exposition of the titanium alloy surface to air and to culture solution. This fact should be mentioned somewhere in the text. As shown in Fig. 12, the cells spread out on the surfaces of the titanium alloy and T–P coating well after culturing 5 days. After 7 days, on the surfaces of the titanium alloy and T–P coating the cells shows smooth and flat morphology and almost contact each other with a small gap among them.

4. Conclusion

T–P coating was formed in the electrolyte containing $(NaPO_3)_6$ and NaOH by MAO. The surface morphology, phase composition and thickness of the T–P coatings are highly dependent on the applied voltage. The Ti, Al, O and P elements show graded distribution along the coating depth. After SBF immersion, the T–P coating formed at 300 V can induce the formation of biomimetic apatite. The MG63 cell proliferation on the surfaces of titanium alloy and the T–P coating formed at 300 V is good.

Acknowledgement

This work was financially supported by National Natural Science Foundation of China (Grant No. 50872025).

References

[1] X.Y. Liu, K.C. Paul, C.X. Ding, Surface modification of titanium, titanium alloys, and related materials for biomedical applications, Mater. Sci. Eng. R 47 (2004) 49–121.
[2] Y.C. Yang, E.W. Chang, B.H. Hwang, S.Y. Lee, Biaxial residual stress states of plasma-sprayed hydroxyapatite coatings on titanium alloy substrate, Biomaterials 21 (2000) 1327–1337.
[3] C.F. Feng, K.A. Khor, E.J. Liu, P. Cheang, Phase transformations in plasma sprayed hydroxyapatite coatings, Scripta Mater. 42 (2000) 103–109.
[4] E. Milella, F. Cosentino, A. Licciulli, C. Massaro, Preparation and characterisation of titania/hydroxyapatite composite coatings obtained by sol–gel process, Biomaterials 22 (2001) 1425–1431.
[5] Q.Y. Zhang, Y. Leng, R.L. Xin, A comparative study of electrochemical deposition and biomimetic deposition of calcium phosphate on porous titanium, Biomaterials 26 (2005) 2857–2865.
[6] D.Q. Wei, Y. Zhou, D.C. Jia, Y.M. Wang, Characteristic and in vitro bioactivity of microarc oxidized TiO_2-based coating after chemical treatment, Acta Biomater. 3 (2007) 817–827.
[7] D.Q. Wei, Y. Zhou, D.C. Jia, Y.M. Wang, Effect of heat treatment on the structure and in vitro bioactivity of microarc-oxidized (MAO) titania coatings containing Ca and P ions, Surf. Coat. Technol. 201 (2007) 8723–8729.
[8] D.Q. Wei, Y. Zhou, D.C. Jia, Y.M. Wang, Effect of applied voltage on the structure of microarc oxidized TiO_2-based bioceramic films, Mater. Chem. Phys. 104 (2007) 177–182.
[9] D.Q. Wei, Y. Zhou, Y.M. Wang, D.C. Jia, Characteristic of microarc oxidized coatings on titanium alloy formed in electrolytes containing chelate complex and nano-HA, Appl. Surf. Sci. 253 (2007) 5045–5050.
[10] D.Q. Wei, Y. Zhou, D.C. Jia, Y.M. Wang, Biomimetic apatite deposited on microarc oxidized anatase-based ceramic coating, Ceram. Int. 34 (2008) 1139–1144.

[11] M. Fini, A. Cigada, G. Rondelli, In vitro and in vivo behaviour of Ca- and P-enriched anodized titanium, Biomaterials 20 (1999) 1587–1594.
[12] X.L. Zhu, K.H. Kim, Y.S. Jeong, Anodic oxide films containing Ca and P of titanium biomaterial, Biomaterials 22 (2001) 2199–2206.
[13] X.L. Zhu, J.L. Ong, S.Y. Kim, K.H. Kim, Surface characteristics and structure of anodic oxide films containing Ca and P on a titanium implant material, J. Biomed. Mater. Res. 60 (2002) 333–338.
[14] Y. Han, S.H. Hong, K.W. Xu, Structure and in vitro bioactivity of titania-based films by micro-arc oxidation, Surf. Coat. Technol. 168 (2003) 249–258.
[15] V.M. Frauchiger, F. Schlottig, B. Gasser, M. Textor, Anodic plasma-chemical treatment of CP titanium surfaces for biomedical applications, Biomaterials 25 (2004) 593–606.
[16] L.H. Li, Y.M. Kong, H.W. Kim, Improved biological performance of Ti implants due to surface modification by micro-arc oxidation, Biomaterials 25 (2004) 2867–2875.
[17] W.H. Song, Y.K. Jun, Y. Han, S.H. Hong, Biomimetic apatite coatings on microarc oxidized titania, Biomaterials 25 (2004) 3341–3349.
[18] W.H. Song, H.S. Ryu, S.H. Hong, Apatite induction on Ca-containing titania formed by micro-arc oxidation, J. Am. Ceram. Soc. 88 (2005) 2642–2644.
[19] H.S. Ryu, W.H. Song, S.H. Hong, Biomimetic apatite induction of P-containing titania formed by micro-arc oxidation before and after hydrothermal treatment, Surf. Coat. Technol. 202 (2008) 1853–1858.
[20] A. Oyane, H.M. Kim, T. Furuya, T. Kokubo, T. Miyazaki, T. Nakamura, Preparation and assessment of revised simulated body fluids, J. Biomed. Mater. Res. A 65 (2003) 188–195.
[21] A.L. Yerokhin, X. Nie, A. Leyland, A. Matthews, S.J. Dowey, Plasma electrolysis for surface engineering, Surf. Coat. Technol. 122 (1999) 73–93.
[22] J.M. Gomez-Vega, E. Saiz, A.P. Tomsia, T. Oku, K. Suganuma, Novel bioactive functionally graded coatings on Ti6Al4V, Adv. Mater. 12 (2000) 894–899.
[23] L. Müller, F.A. Müller, Preparation of SBF with different HCO_3^- content and its influence on the composition of biomimetic apatites, Acta Biomater. 2 (2006) 181–189.
[24] S. Koutsopoulos, Synthesis and characterization of hydroxyapatite crystals: a review study on the analytical methods, J. Biomed. Mater. Res. 62 (2002) 600–612.
[25] G.K. Toworfe, R.J. Composto, I.M. Shapiro, P. Ducheyne, Nucleation and growth of calcium phosphate on amine-, carboxyl- and hydroxyl-silane self-assembled monolayers, Biomaterials 27 (2006) 631–642.
[26] H.M. Kim, F. Miyaji, T. Kokubo, T. Nakamura, Preparation of bioactive Ti and its alloys via simple chemical surface treatment, J. Biomed. Mater. Res. 32 (1996) 409–417.
[27] X.X. Wang, S. Hayakawa, K. Tsuru, A. Osaka, Improvement of bioactivity of $H_2O_2/TaCl_5$-treated titanium after subsequent heat treatments, J. Biomed. Mater. Res. 52 (2000) 171–176.
[28] X.X. Wang, S. Hayakawa, K. Tsuru, A. Osaka, Bioactive titania gel layers formed by chemical treatment of Ti substrate with a H_2O_2/HCl solution, Biomaterials 23 (2002) 1353–1357.
[29] Q. Liu, J. Ding, F.K. Mante, S.L. Wunde, G.R. Baran, The role of surface functional groups in calcium phosphate nucleation on titanium foil: a self-assembled monolayer technique, Biomaterials 23 (2002) 3103–3111.
[30] T. Kokubo, H.-M. Kim, M. Kawashita, Novel bioactive materials with different mechanical properties, Biomaterials 24 (2003) 2161–2175.
[31] A.L. Oliveira, J.F. Mano, R.L. Reis, Nature-inspired calcium phosphate coatings: present status and novel advances in the science of mimicry, Curr. Opin. Solid-State Mater. Sci. 7 (2003) 309–318.
[32] H.M. Kim, Ceramic bioactivity and related biomimetic strategy, Curr. Opin. Solid-State Mater. Sci. 7 (2003) 289–299.
[33] T. Kawai, C. Ohtsuki, M. Kamitakahara, T. Miyazaki, Coating of an apatite layer on polyamide films containing sulfonic groups by a biomimetic process, Biomaterials 25 (2004) 4529–4534.
[34] K. Duan, R.Z. Wan, Surface modifications of bone implants through wet chemistry, J. Mater. Chem. 16 (2006) 2309–2321.
[35] T. Hanawa, M. Kon, H. Doi, Amount of hydroxyl radical on calcium-ion-implanted titanium and point of zero charge of constituent oxide of the surface-modified layer, J. Mater. Sci. Mater. Med. 9 (1998) 89–92.
[36] W. Wu, G.H. Nancollas, Nucleation and crystal growth of octacalcium phosphate on titanium oxide surfaces, Langmuir 13 (1997) 861–865.
[37] D.Q. Wei, Y. Zhou, Y.M. Wang, D.C. Jia, Chemical etching of micro-plasma oxidized titania film on titanium alloy and apatite deposited on the surface of modified titania film in vitro, Thin Solid Film 516 (2008) 1818–1825.